# Imaging Sgr A* through time-variability

R.-S. Lu[1,2], F. Roelofs[3], V. F. Fish[1], S. S. Doeleman[1], H. Shiokawa[4], C. F. Gammie[4], and H. Falcke[3]

[1]MIT Haystack Observatory, Westford, MA, USA [2]Max Planck Institute for Radio Astronomy, Bonn, Germany
[3]Radboud University, Nijmegen, The Netherlands [4]University of Illinois, Urbana, IL, USA

## Introduction

Recent general relativistic magnetohydrodynamic (GRMHD) simulations have shown that 1.3 mm emission from Sgr A* exhibits variability on a timescale of minutes. The static source assumption in interferometric theory is thus violated for Sgr A*. In this work, a method to nonetheless obtain an image of the average quiescent structure of Sgr A* has been developed.

## Simulating EHT observations with MAPS

EHT observations of a GRMHD movie of Sgr A* have been simulated with the MIT Array Performance Simulator (MAPS) following Lu et al. (2014). MAPS is a simulator work package that can generate interferometric data sets from a model image and observational parameters. The process is explained in Figure 1. The assumed array is shown in Figure 2.

Sgr A* was observed for several days, after which visibilities with equal $(u, v)$ coordinates were averaged. For comparison, a one-day observation of the average image of all movie frames as a static source was simulated.

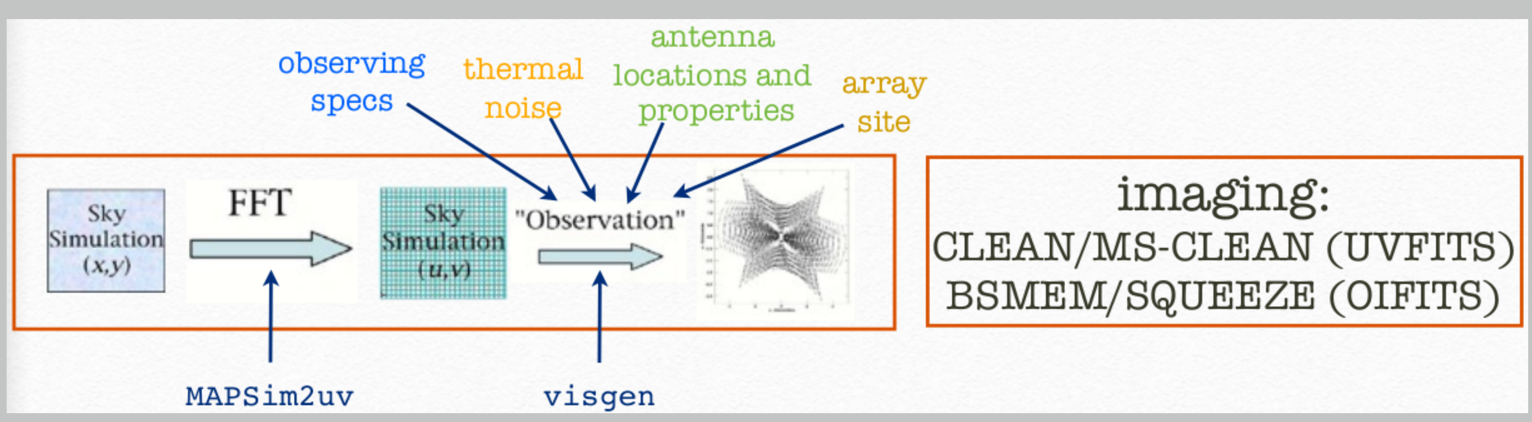


Figure 1 : Schematic overview of the steps executed in MAPS to reconstruct an input brightness distribution. The input is first Fourier transformed (`MAPSim2uv`) before visibilities are generated in the $(u, v)$ plane (`visgen`), depending on the observational parameters. These can then be imaged with imaging softwares.


Figure 2 : Array used to reconstruct observations of a movie of Sgr A*. Image modified from EHT collaboration (2013).

## Additional methods: scaling and smoothing

As shown in Figure 3 (upper plot), the averaged visibilities (blue) are still different from the visibilities obtained from the static image (red). To correct for this, all visibility amplitudes were divided by the total flux density of the currently observed frame, so that they were normalized (middle plot). Then, a smoothing algorithm was applied (lower plot). To simulate the effects of interstellar scattering, all movie frames were convolved with the best-bet scattering kernel from Bower et al. (2006). All visibilities were then divided by the Fourier transform of the scattering kernel following Fish et al. (2014).

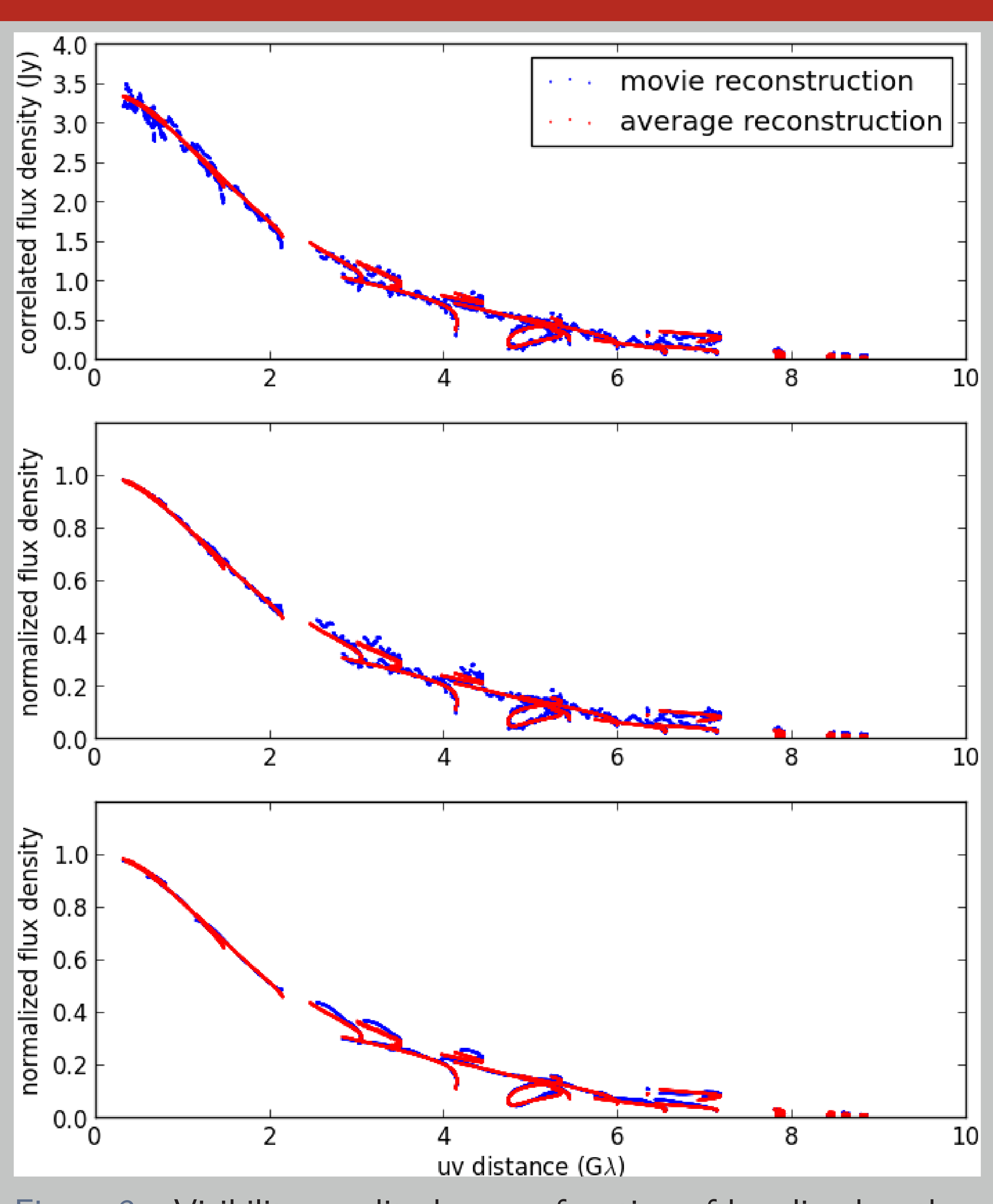


Figure 3 : Visibility amplitudes as a function of baseline length for the averaged output of an eight-day MAPS simulation (blue, upper), after scaling (blue, middle) and after smoothing (blue, lower). For comparison, visibility data for a one-day observation of the average of all movie frames as a static source was added (red).

## Results

Figure 4a shows the average image of all movie frames. Figures 4b and 4c are reconstructions of this average image (without and with considering interstellar scattering effects) as a static source. Figures 4d through 4l are reconstructions of the movie, made for several combinations of observing time, scaling, smoothing, and (correcting for) interstellar scattering, as indicated in Table 1. All reconstructions were compared to the movie average using two image quality metrics. MSE is a pixel-by-pixel comparison, while DSSIM is based on theories of human visual perception (Loza et al., 2009). Lower metric values indicate more resemblance with the movie average.

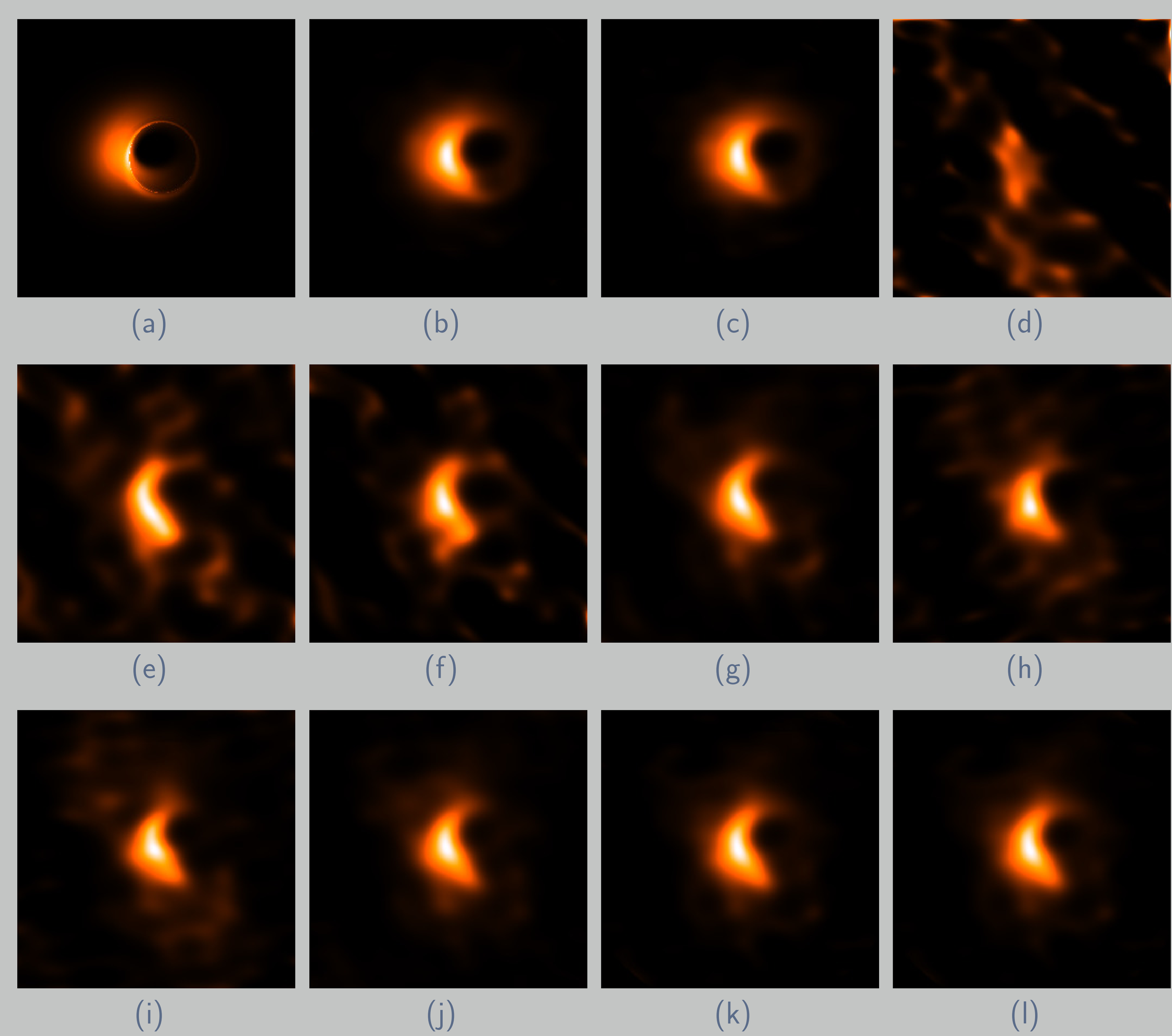


Figure 4 : Average image of all movie frames (a) and images of combinations in Table 1 (b-l).

Table 1 : MSE and DSSIM metric values for several reconstructions of the movie. Lower values indicate more resemblance with the average image of all movie frames. Images shown in Figure 4.

| Image | Observed | Scaled by total flux of frame | Smoothed | Scattered and deblurred | MSE | DSSIM |
|---|---|---|---|---|---|---|
| b | Static | n | n | n | 0.0449 | 0.0532 |
| c | Static | n | n | y | 0.0451 | 0.0544 |
| d | 1 day | n | n | n | 0.5680 | 0.4627 |
| e | 1 day | y | y | n | 0.2163 | 0.8032 |
| f | 1 day | y | y | y | 0.1365 | 0.3244 |
| g | 4 days | y | y | y | 0.1067 | 0.2755 |
| h | 8 days | n | n | y | 0.1265 | 0.4452 |
| i | 8 days | n | y | y | 0.1554 | 0.5456 |
| j | 8 days | y | n | y | 0.0924 | 0.2311 |
| k | 8 days | y | y | y | 0.0766 | 0.1535 |
| l | 8 days | y | y | n | 0.0754 | 0.1504 |

## Conclusions

- **An image of the average quiescent structure of Sgr A* showing the black hole shadow and photon ring can be obtained, despite its variability.**
- **The reconstruction quality increases as the observing time is increased and scaling and smoothing are applied.**
- **If the scattering kernel is known, the reconstructions can be corrected well for interstellar scattering.**

## References

Bower, G. C., Goss, W. M., Falcke, H., Backer, D. C., and Lithwick, Y. (2006). The Intrinsic Size of Sagittarius A* from 0.35 to 6 cm. *ApJL*, 648:L127–L130.

Fish, V. L., Johnson, M. D., Lu, R.-S., Doeleman, S. S., Bouman, K. L., Zoran, D., Freeman, W. T., Psaltis, D., Narayan, R., Pankratius, V., Broderick, A. E., Gwinn, C. R., and Vertatschitsch, L. E. (2014). Imaging an Event Horizon: Mitigation of Scattering toward Sagittarius A*. *ApJ*, 795:134.

Loza, A., Mihaylova, L., Bull, D., and Canagarajah, N. (2009). Structural similarity-based object tracking in multimodality surveillance videos. *Machine Vision and Applications*, 20:71.

Lu, R.-S., Broderick, A. E., Baron, F., Monnier, J. D., Fish, V. L., Doeleman, S. S., and Pankratius, V. (2014). Imaging the Supermassive Black Hole Shadow and Jet Base of M87 with the Event Horizon Telescope. *ApJ*, 788:120.

EHT collaboration (2013). Building a larger array. `http://www.eventhorizontelescope.org/technology/building_a_larger_array.html`.

rslu@mpifr-bonn.mpg.de